SKY IMAGE LICENSED BY GRAPHIC STOCK. HIKER IMAGE ©ISTOCKPHOTO.COM/KENCORD4

# Walking Assistance Using Artificial Primitives

## *A Novel Bioinspired Framework Using Motor Primitives for Locomotion Assistance Through a Wearable Cooperative Exoskeleton*

By Virginia Ruiz Garate, Andrea Parri, Tingfang Yan, Marko Munih, Raffaele Molino Lova, Nicola Vitiello, and Renaud Ronsse

Bioinspiration in robotics deals with applying biological principles to the design of better performing devices. In this article, we propose a novel bioinspired framework using motor primitives for locomotion assistance through a wearable cooperative exoskeleton. In particular, the use of motor primitives for assisting different locomotion modes (i.e., ground-level walking at several cadences and ascending and descending stairs) is explored by means of two different strategies. In the first strategy, identified motor primitives are combined through weights to directly produce the desired assistive torque profiles. In the second strategy, identified motor primitives are combined to serve as neural stimulations to a virtual model of the musculoskeletal system, which, in turn, produces the desired assistive torque profiles.

This article further reports the results of an experiment conducted with healthy participants, where the proposed

*Digital Object Identifier 10.1109/MRA.2015.2510778*
*Date of publication: 23 February 2016*

strategies were tested for the first time with a wearable robotic exoskeleton for hip assistance. Several volunteers performed the task of ground-level walking in different conditions. These experimental activities highlighted the capacity of volunteers to naturally interact with the device and benefit from the assistance in terms of physical effort.

## Bioinspired Locomotion Assistance

Aging among populations is a critical challenge for industrialized countries. In 40 years, nearly 21% of the European population will be older than 60 years [1]. Therefore, it is urgent to develop new technologies that promote the establishment of an active and sustainable aging society. The incidence of gait disorders and lower-limb impairments is higher among aged people and can reach 35 and 60% prevalence in persons over 70 and 80 years of age, respectively [2]. This scenario is expected to lead to an increasing number of people with gait disturbances (e.g., senile gait, gait poststroke hemiparesis, and lower-limb amputations) who may benefit from the use of lightweight, assistive wearable robots to recover a more stable, efficient, and autonomous locomotion [3], [4].

**EMG-driven devices face the problem of deploying a complex and sensitive sensory apparatus.**

Several wearable robots for lower-limb movement assistance can be found in the literature. However, despite the tremendous work carried out by engineers, many challenges regarding the design of an effective physical and cognitive human–robot interface still remain.

In this framework, a compelling research topic is the development of an adaptive, robust, and intuitive control strategy to decode the intended movement of users with mild lower-limb impairment and smoothly provide them with coherent and collaborative assistance. An extensive review of such devices and their control strategies can be found in [5] and [6]. Hereafter, we recap the most relevant approaches and their major limitations.

Several authors explored the use of superficial electromyographic signals (EMGs) to generate assistive torques [7]. However, EMG-driven devices face the problem of deploying a complex and sensitive sensory apparatus and require advanced and computationally greedy signal processing to filter out measurement noise and signal instability [8]. Furthermore, laborious tuning is needed for each subject and even training session.

In other seminal contributions, the estimate of the assistive torque was derived from the computation of a dynamic model of the exoskeleton or the exoskeleton-human complex [9]. This approach mostly suffers from the lack of accuracy of the model, the heavy computational load, and the need to deal with the identification of as many different dynamic models as the number of users.

A promising approach that has been recently introduced gets inspiration from the so-called central pattern generators (CPGs), i.e., neural oscillators located in the spinal cord of mammals. CPGs are considered as the source of rhythmicity in locomotion due to their capability of providing rhythmic excitation to the muscles, even if receiving nonperiodic inputs [10], [11]. Based on this idea, adaptive oscillators (AOs) were proposed as mathematical tools to extract the periodic characteristics of locomotion and, therefore, emulate the role of CPGs as neural oscillators. AOs are coupled to user movements so that they provide the necessary entrainment between the device and the user by delivering appropriate assistive patterns [3], [12], [13]. In some cases, AOs were used to adapt prerecorded trajectories or torque profiles to the user gait pattern, which implied adding more profiles every time a new maneuver is programmed [3]. Other contributions explored the ability of AOs to synchronize with and learn the monitored gait pattern to enhance the user gait by means of virtual impedance fields [13]. Such approaches are prone to find difficulties while transitioning from one locomotion mode to another, e.g., changing from walking to ascending stairs.

In this article, we propose an innovative bioinspired framework that further exploits the concept of CPGs by combining AOs with artificial motor primitives for the development of a control strategy to assist locomotion through a wearable cooperative exoskeleton.

Physiologically speaking, motor primitives can be defined as a network of spinal neurons that form one basic module that activates a determined set of muscles. In other words, they are a set of basic signals that, through proper recombination, are able to generate the large set of muscle stimulations needed for different locomotion tasks. The existence of these primitives has been widely studied and supported by contributions like [16] and [17], in which Bizzi et al. reviewed the experiments establishing that five time-varying signals could explain the EMG recordings of 13 leg muscles in three intact frogs during swimming, jumping, and walking. Similarly, in humans, the work of [18] and [19] identified five to six basic components that could reconstruct all the measured EMG signals for several locomotion tasks, such as walking and running at different speeds. Though these studies mainly focused on EMG recordings, similar correlations of signals have also been found at other levels, i.e., neural, dynamic, and kinematic levels [17], [20].

Such primitives present several potential advantages for motor control. First, inferring high-dimensional sets of data from a small set of simple signals provides an advantageous reduction in dimensionality [11]. In addition, this reduced set of primitives also implies a simplification of the coordination, since a reduced number of control signals is used to trigger them with the appropriate combination. Moreover, this combination is done linearly, which provides an efficient way to bypass the inherent nonlinearities that govern movement control [11].

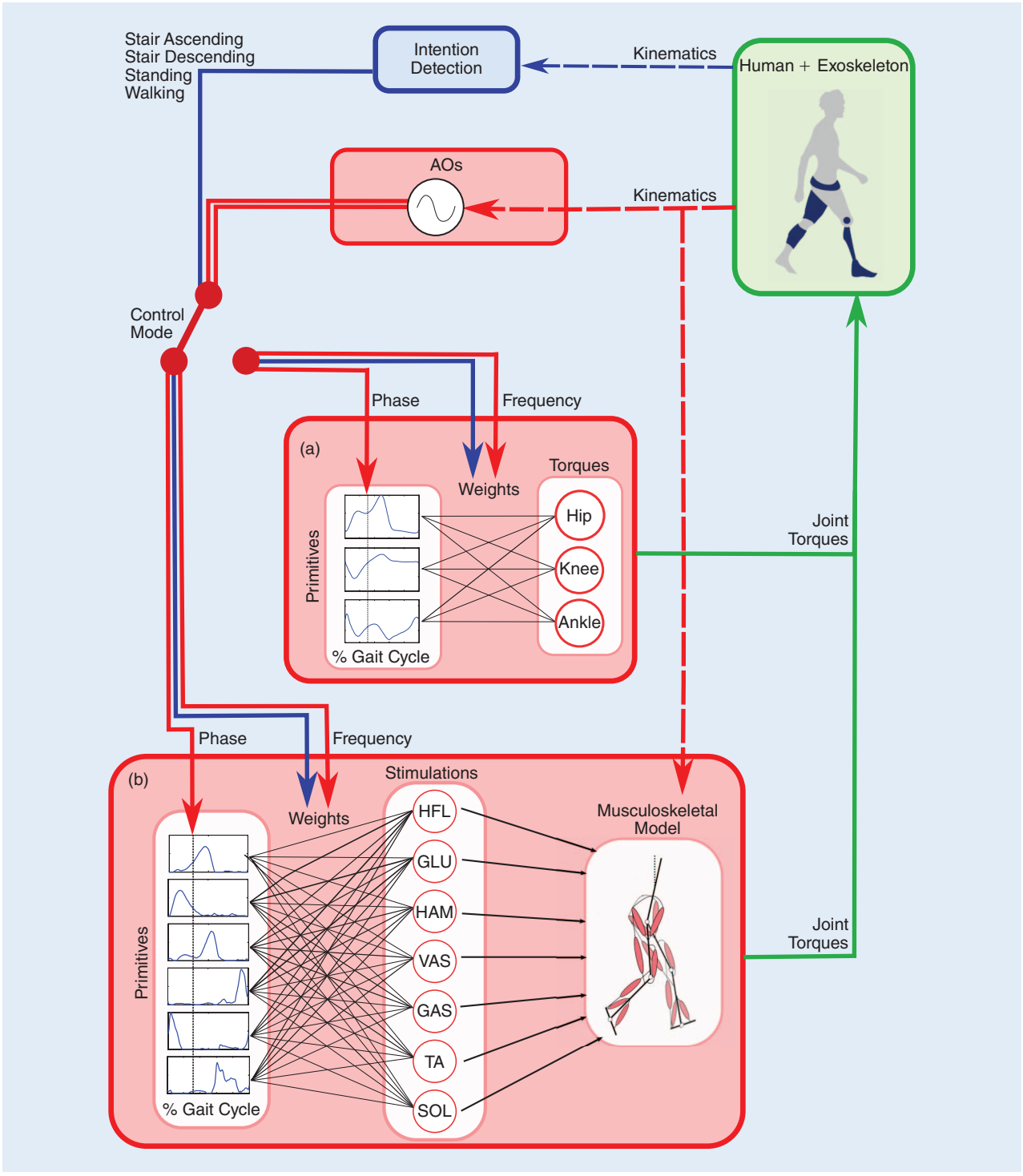


**Figure 1.** A bioinspired controller: (a) a controller based on dynamic primitives (DLMPs) and (b) a controller based on neural primitives (NLMPs). The components of the developed controllers (AOs and primitive-based controllers) are shown in red. The blue box represents the algorithm detecting the motor intention of the user. The green box represents the human–orthosis coupled system. HFL: hip flexor; GLU: gluteus; HAM: hamstring; VAS: vastus; GAS: gastrocnemius; TA: tibialis anterior; SOL: soleus.

These advantages make the physiological concept of motor primitives an inspiring foundation for the control of artificial devices such as orthoses, prostheses, and even autonomous robots. These devices may benefit from a primitive-based control in complex environments where different locomotion modes are requested [21]. Furthermore, the use of the same reduced set of primitive signals for different locomotion tasks presents the desirable advantage of generating smoother transitions between them.

In this article, the generation of artificial primitives is studied at two different levels, the dynamic and neural levels. The controller based on dynamic-level primitives combines a set of

basic signals to directly generate desired torque profiles. In the case of the neural level, a further step toward bioinspiration is taken, in the sense that primitives are combined to produce virtual muscle stimulations. Therefore, a musculoskeletal model is needed to turn these stimulations into desired joint torques. In both strategies, AOs are used to continuously synchronize the primitives to the subject's instantaneous walking cadence, allowing for adaptation to diverse gait frequencies and phases [22].

## Primitive-Based Control

The proposed assistive strategy based on both dynamic-level artificial motor primitives (DLMPs) and neural-level artificial motor primitives (NLMPs) is shown in Figure 1.

Common blocks of both strategies include the following: 1) the intention detection, which monitors the subject's behavior to select among the different locomotion modes, i.e., standing, walking, and ascending/descending stairs; and 2) the AOs, which are in charge of estimating the gait frequency (cadence) and phase for each leg independently. These features are necessary to select the appropriate combination of primitives in a coordinated timing. On the other hand, the strategies differ as follows. In the case of the control strategy based on DLMP [Figure 1(a)], primitives are combined with different weights to generate the desired joint torque profiles for the hip, knee, and ankle. Otherwise, the control based on NLMP [Figure 1(b)] combines a different set of primitives to generate muscle stimulations. These stimulation signals enter a simplified musculoskeletal model comprising seven muscle–tendon units based on Hill-type muscles adapted from [14]. This model transforms the stimulations into muscle–tendon forces and finally projects them into joint torques. Therefore, the NLMP-based control is also dependent on the actual kinematics of the subjects, and it is thus adaptive to their natural gait pattern. With this bidirectional adaptation, the subject can better exploit the assistive potential by also adapting his or her gait to optimize the received assistance [15].

**This, together with the direct torque control output, makes the proposed control approach easily transferable to any torque-controlled assistive robot.**

We computed both sets of motor primitives (DLMPs and NLMPs) for three locomotion tasks: walking and ascending and descending stairs. With this aim, a database was constructed by collecting data from different references, providing kinematics and dynamics in the sagittal plane of walking at different cadences and ascending and descending stairs (see Table 1). These contributions provide a single set of signals for both legs, assuming a symmetrical gait in healthy subjects.

To simplify the primitive-extraction process, the stair data were averaged, and walking signals were grouped and averaged in five bins of walking cadences, i.e., (0.6–0.69), (0.7–0.79), (0.8–0.89), (0.9–0.99), and (1–1.09) Hz. These signals were further normalized with respect to time as the percentage of gait cycle (0–100%, with 0% being coincident with the corresponding leg heel strike). Computations were performed using custom software routines (MATLAB R2013a, The MathWorks Inc., Natick, Massachusetts, United States).

**Table 1. An overview of the literature data used for generating the primitives.**

| Reference | Locomotion Task | Cadences (Hz) | Number of Subjects |
|---|---|---|---|
| Winter, 1991 [23] | Walking | 0.72 | 19 |
| | | 0.88 | 19 |
| | | 1.03 | 17 |
| Wang et al., 2012 [24] | Walking | 0.82 | 5 |
| | | 0.91 | 5 |
| | | 0.98 | 5 |
| | | 1.04 | 5 |
| Koopman et al., 2010 [25] | Walking | 0.6 | 4 |
| | | 0.7 | 5 |
| | | 0.8 | 8 |
| | | 0.9 | 3 |
| Bradford et al., 1988 [26] | Ascending stairs | — | 3 |
| | Descending stairs | | 3 |
| Riener et al., 2002 [27] | Ascending stairs | — | 10 |
| | Descending stairs | | 10 |

Then, the primitives were extracted with techniques, such as a nonnegative matrix factorization (NNMF) or a principal component analysis (PCA). Both of these techniques extract a linear combination of primitives $C$ and the corresponding weights $W$ to minimize the difference between the original signals and the reconstructed ones $S$:

$$S_{e,t} = W_{e,n} \cdot C_{n,t}, \tag{1}$$

where $t$ denotes the sample times (in our case, normalized from 0 to 100% of the gait cycle), $n$ is the number of primitives, and $e$ is the number of reconstructed signals, depending on the number of gait patterns and cadences to be considered and on the level of organization of the primitives (DLMPs or NLMPs).

### *Dynamic-Level Primitives*

In this case, the objective was to find the minimum set of primitives that can directly reconstruct all leg joint torque profiles from the data set (Table 1). Three sagittal joint torques—hip, knee, and ankle—were extracted for seven different conditions: five different walking cadences and ascending and descending stairs. These torques are displayed in the left panel of Figure 2(a).

The decomposition process relied on PCA. From its outcome, we kept the number of components necessary to account for at least 95% of the variance. We further assessed

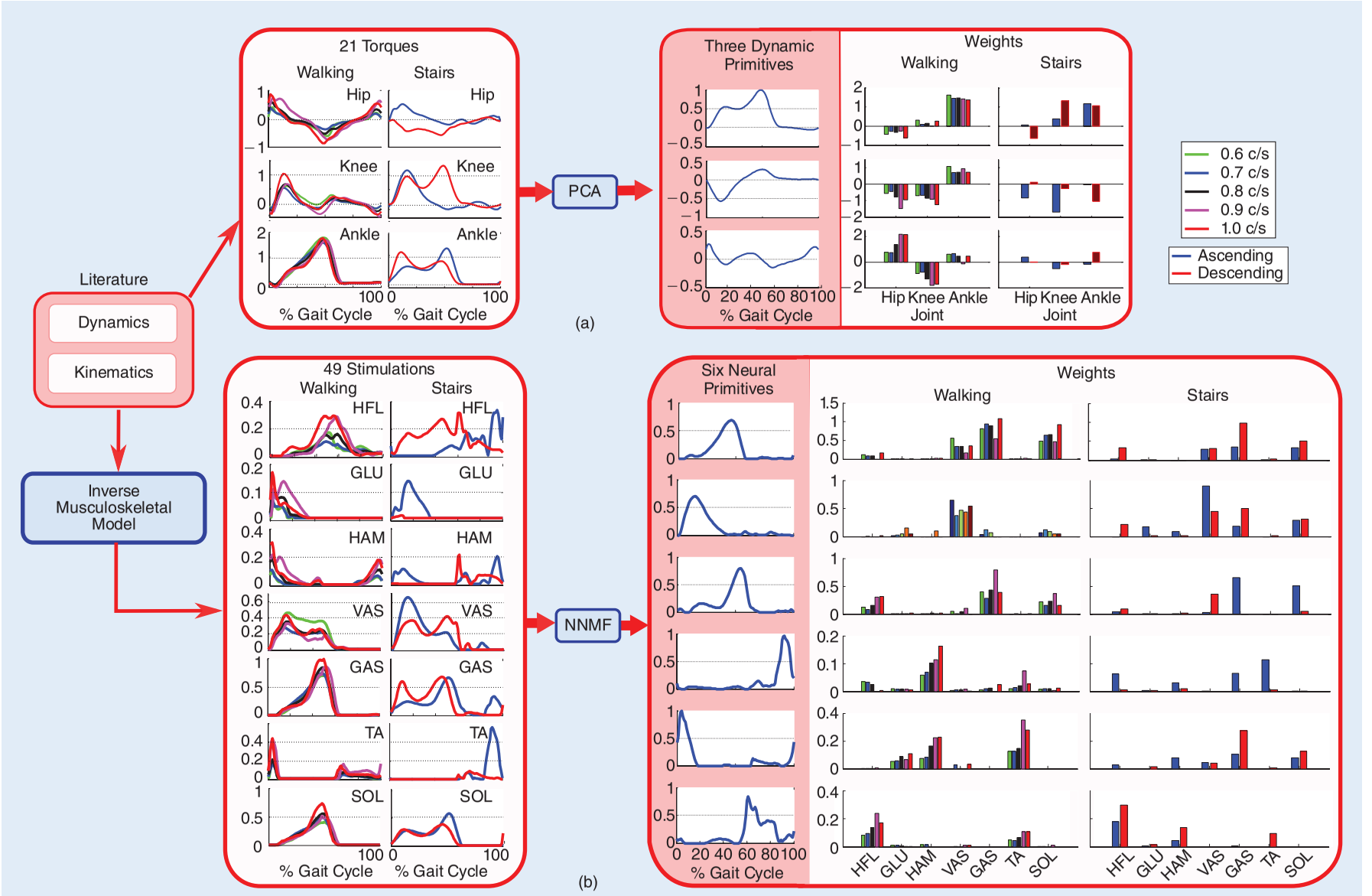


**Figure 2.** The primitive extraction process: (a) DLMP extraction from the literature torque data by means of PCA and (b) NLMP extraction. Muscle stimulations are obtained by an inverse musculoskeletal model using kinematic and torque data from the literature. Neural primitives are then obtained from these muscle stimulations by NNMF. In (a) and (b), for each component, the walking bar graph represents the weight evolution of primitives for the different joint torques (DLMPs) or muscle stimulations (NLMPs) as a function of the walking cadence. The bar graph on the right represents the corresponding weights in the case of ascending (blue) and descending (red) stairs.

the performance of the selected primitives by computing the normalized root-mean-square error and added components until this error became less than 4% between the reconstructed and actual signals. Only three primitives were necessary to account for approximately 98% of the data set total variance.

**These devices may benefit from a primitive based control in complex environments where different locomotion modes are requested.**

These selected primitives are displayed in the right panel of Figure 2(a) along with the corresponding weights to reconstruct the original data. Finally, the weights for the different walking cadences were simplified by fitting their evolution using second-order polynomials.

### Neural-Level Primitives

In this case, the objective was to find the minimum set of components to reconstruct all possible muscle stimulations. Hereafter, the selected musculoskeletal model is described. Next, we explain how the muscle stimulations used to activate the model were obtained from the data in Table 1. Finally, the method to identify the target set of artificial motor primitives is presented.

The musculoskeletal model was implemented based on the one developed by [14], comprising seven virtual muscle-tendon units per leg. Each unit captures the following leg muscle groups (Figure 3):

- *hip flexor (HFL) muscle*: monoarticular hip flexor
- *gluteus (GLU) muscle*: monoarticular hip extensor
- *hamstring (HAM) muscle*: biarticular knee flexor and hip extensor
- *vastus (VAS) muscle*: monoarticular knee extensor
- *gastrocnemius (GAS) muscle*: biarticular ankle plantar flexor and knee flexor
- *tibialis anterior (TA) muscle*: monoarticular ankle dorsiflexor
- *soleus (SOL) muscle*: monoarticular ankle plantar flexor.

These muscle–tendon units are modeled as Hill-type muscles [Figure 3(a)]: the force $F_m$ being generated by a muscle results from the interaction between a series elastic element (SE), a parallel element (PE), a buffer elasticity (BE) preventing the muscle from collapsing, and the active contractile element (CE) [14]. The force generated by the CE depends on $l_{CE}$ and its first derivative $v_{CE}$, i.e., the muscle length and contraction velocity, respectively, capturing the force–length and force–velocity relationships of a biological muscle.

This model thus introduces a local force feedback in the muscle–tendon unit based on muscle length and velocity. This feedback, together with the serial and parallel elasticities, plays a significant role to endow the muscle unit with an intrinsically nonzero impedance and enhance its stability. Afterward, these muscle forces are converted into muscle torques through geometrical relationships: $\tau_m = r_m \cdot F_m$, where $r_m$ corresponds to the lever arm of the muscle attachment point [14]. Finally, the muscle model computes the joint torques as a function of the torque provided by each muscle:

$$\begin{aligned} \tau_{\text{HIP}} &= \tau_{\text{HAM}} + \tau_{\text{GLU}} - \tau_{\text{HFL}} + \tau_{lH} \\ \tau_{\text{KNEE}} &= \tau_{\text{VAS}} - \tau_{\text{GAS}} - \tau_{\text{HAM}} + \tau_{lK} \\ \tau_{\text{ANKLE}} &= \tau_{\text{SOL}} + \tau_{\text{GAS}} - \tau_{TA} + \tau_{lA}, \end{aligned} \tag{2}$$

where $\tau_{lH}$, $\tau_{lK}$, and $\tau_{lA}$ are torques preventing the hip, knee, and ankle, respectively, from reaching their physical limits [14]. Numerical parameters of the muscle units and of the skeleton geometry were taken from the ones in [14], pending some adaptations to the subjects, anthropometry (see the "Experimental Validation" section).

Neural primitives reconstruct muscle stimulations. Therefore, these target muscle stimulations have first to be computed from the available kinematic and dynamic data (Table 1) before computing the corresponding primitives. For this purpose, an inverse model of the introduced musculoskeletal model was created and scaled depending on the anthropometry reported for each data set. The outcome of this stimulation computation is displayed in the left panel of Figure 2(b).

To get a reduced set of primitives that could reconstruct all these muscle stimulations, NNMF was performed. Because NNMF may converge to local minima, the process was repeated 100 times, and the one with the lowest residual error was kept as the solution.

As input to the NNMF process, there were seven muscle stimulations for seven different conditions: the five different walking cadences and ascending and descending stairs. In coherence with the first decomposition, the first primitives were kept up to accounting for at least 95% of the variance and less than 4% of reconstruction error. This led to six components, which also accounted for around 98% of the variance [see the right panel of Figure 2(b)].

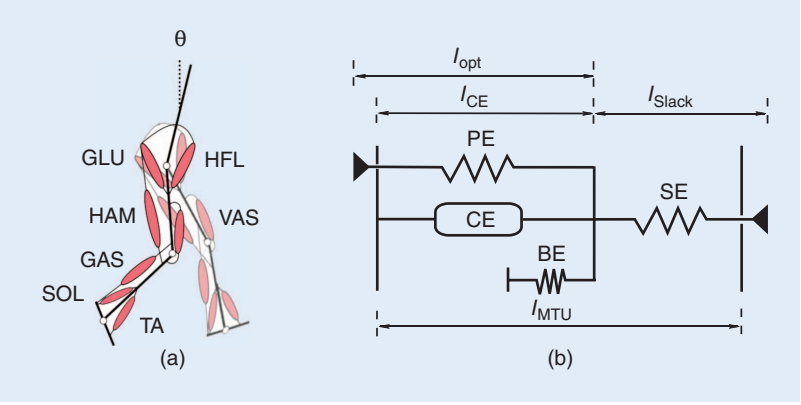


**Figure 3.** (a) The seven main muscle groups actuating one leg. (b) The Hill-type muscle. (Figure adapted from [14].)

Many of the stimulations actually received a negligible contribution for some of the primitives (i.e., several weights were very close to zero). Any coefficients that were at least ten times smaller than the most influential one were rounded to zero. In addition, the weight evolutions across the five walking cadences were interpolated using second-order polynomials.

Interestingly, the number of significant primitives found is similar to the literature reports that extracted primitives from real EMG data [18], [19]. In these studies, the authors took a larger number of muscles into account. However, they analyzed mainly walking and running, while we introduce very different locomotion modes, that is, ascending and descending stairs.

**Table 2. The participants' features and trial ordering.**

| Subject | Gender | Age | Weight (kg) | Order of Assistive Trials |
|---|---|---|---|---|
| S1 | Male | 30 | 85 | TM – LTA – HSA – LSA – HTA – NO |
| S2 | Male | 30 | 76 | TM – LSA – LTA – HSA – HTA – NO |
| S3 | Male | 27 | 87 | TM – LSA – LTA – HSA – HTA – NO |
| S4 | Female | 35 | 68 | TM – LTA – HSA – HTA – LSA – NO |
| S5* | Female | 33 | 66 | NO – LSA – TM – LTA – HSA – NO – HTA |
| S7 | Male | 35 | 82 | NO – LTA – HTA – LSA – HSA – TM |
| S9 | Male | 22 | 73 | NO – LTA – HTA – TM – LSA – HSA |

*For this subject, a technical issue caused the recording to stop before the last trial. An extra session was thus organized, with HTA as a unique assisted trial, along with an extra NO trial for normalization of oxygen uptake.

## Experimental Validation

A preliminary validation experiment of the primitive-based controller was conducted, focusing on the walking maneuver. To deliver the desired assistive torques, the active pelvis orthosis (APO) developed within the CYBERLEGs project was used [28]. This device is an advanced version of a previous laboratory prototype presented in [29]. It has two actuation units that employ a series elastic actuator to actively drive the hip flexion/extension movement of each leg. (The design of this actuation system is under patent application: "Sistema di Attuazione per Ortesi di Anca," Italian patent application FI/2015/A/000025.) Consequently, assistance was provided to both hips for flexion/extension, while the computed assistive torques for the knee and ankle were not delivered to the participants. The APO weighs about 8.5 kg. It was used as a stand-alone device in this experiment, although it was originally designed to be coupled to a leg exoskeleton and/or a prosthesis, which could directly transfer part of its weight to the ground. Consequently, it embeds the electronics and battery for actuating more joints than the hip only, explaining why it is heavier than concurrent solutions.

Tests were conducted with both proposed bioinspired methods: the DLMP-based control with direct torque outputs [Figure 1(a)] and the NLMP-based control coupled to the musculoskeletal layer [Figure 1(b)]. A fraction of the desired assistive torques generated by either method was delivered to the joints as a function of the desired level of assistance.

In the case of the NLMP, the musculoskeletal model was adapted to each subject. To do so, numerical parameters of the muscle units and of the skeletal model were scaled as a function of the subject's anthropometry. The muscles attachment lever, optimal, and slack lengths were modulated proportionally to the subject's height, while the maximal isometric force was modulated proportionally to the square of the height.

Furthermore, to assist the participants with the appropriate torque profiles (i.e., the appropriate combination of the primitives and set of weights), it was necessary to infer their motor intention. This was achieved by using a wearable sensory apparatus (WSA) and the methods reported in [30].

To synchronize the control primitives with the actual gait phase of the subject, AOs were used [22], [31]. In this experiment, the hip angles were used as the oscillators' inputs, providing the walking frequency (i.e., the gait cadence in hertz) and the instantaneous phase of each leg (see Figure 1). The same primitives were used for both legs, while a separate AO was used for each side. Consequently, the movement phase and frequency were independently detected for each leg and synchronized to the corresponding heel-strike instants. This approach allowed the delivery of nonsymmetrical torque profiles, since the leg frequencies were not constrained to be equal, and the heel-strike dephasing was not constrained to be 180°.

**The NLMP approach should be more convenient for patients with pathologies causing the natural way of walking to differ from the ideal one of healthy subjects.**

### *Participants*

Nine healthy participants (S1–S9) took part in the experiment: two females and seven males. The participants were between 22 and 35 years old and weighed between 66 and 85 kg. The participants signed a written consent form before starting the experiments. Two subjects were discarded from the analyses due to problems in oxygen consumption recordings: S8 because of technical issues and S6 because he adopted a highly inconsistent behavior across the assisted trials. In particular, he increased and decreased his walking speed in some of the assisted trials by 10–20%. This led to a high impact on his metabolic consumption, which significantly increased. All the other subjects (including S8) walked consistently across trials.

Table 2 shows the seven remaining participants' features and trials ordering. For the assistive order nomenclature, see the "Experimental Protocol" section.

### Experimental Setup

During the experiments, assistance was provided to the hips through the APO device worn by the subjects. A person wearing the full experimental setup is shown in Figure 4. In the figure, the following elements are visible: APO, WSA, and Oxycon Mobile.

**The DLMP-based approach provided larger flexion torque than the NLMP-based approach.**

To evaluate the optimal assistance level and the difference between both assistive methods with respect to the transparent mode (TM), the following data were collected during the experiments.

- The position, velocity, and acceleration of the body segments from the inertial measurement units (IMUs) of the WSA (Figure 4). The IMUs are wireless, battery-powered, and enclosed into a small casing appropriate for attachment on body segments. The IMUs were placed on both shoes, shanks, and tights, and one was placed on the back.
- Ground reaction forces from sensorized insoles of the WSA (Figure 4).
- Oxygen uptake rate $O_2$ from a portable Oxycon Mobile (Carefusion, St. Albans, the United Kingdom) with a sampling time of 5 s (Figure 4).

Moreover, the following data were computed in real time and recorded for offline analyses: gait phase and cadence of each leg from the oscillators, reference joint torques generated by the controller, and actual hip torque and power provided by the APO.


**Figure 4.** The frontal view of a person wearing the experimental setup. The following components are visible: Oxycon Mobile, APO, the sensory system with IMUs, and the shoes instrumented with custom pressure-sensitive insoles. For more details on the latter two, see [30]. (Photos courtesy of Virginia Ruiz Garate.)

### Experimental Protocol

Several subcases were evaluated depending on the type and level of provided assistance. Assistance was provided with two different methods: through direct torques using DLMP or through NLMP and the use of the musculoskeletal model.

Before starting the experiment, each subject underwent a phase of familiarization that lasted around 10 min. During this phase, the subject walked on a treadmill at a self-selected speed, while assistive torques were provided through the pelvis module using both methods. This phase aimed at establishing an estimate of the percentage of assistance to be provided to have similar torque magnitudes for both methods and across subjects. In any case, a saturation of 15 Nm was applied for safety reasons.

Afterward, all subjects underwent a series of 6-min walking tests (WTs) with trials under the following conditions:

- *No APO (NO)*—ground-level walking without wearing the orthosis. It served as a basis for the kinematics and dynamics comparison and to evaluate the natural cadence and oxygen cost during normal walking.
- *APO in TM*—ground-level walking wearing the APO. The APO was controlled in TM, i.e., rendering zero impedance. This condition served to evaluate the influence of wearing the pelvis module on the natural kinematics, dynamics, cadence, and oxygen cost.
- *Low assistance (LA)*—ground-level walking wearing the APO while providing assistance. This condition was applied twice: a walking trial while providing assistance directly by outputting torques [low torque-based assistance (LTA)] and a walking trial while providing assistance through the musculoskeletal model [low stimulation-based assistance (LSA)]. During LA, assistive peak torques were in the range between 2 and 4 Nm.
- *High assistance (HA)*—ground-level walking wearing the APO while providing assistance. This condition was applied twice: a walking trial while providing assistance directly by outputting torques [high torque-based assistance (HTA)] and a walking trial while providing assistance through the musculoskeletal model [high stimulation-based assistance (HSA)]. During HA, assistive torques were in the range between 4 and 6 Nm.

Importantly, subjects performed these trials by walking in a free environment, i.e., not on a treadmill. Specifically, they

walked back and forth along a corridor of 30 m without stopping at the turns. At the end of each turn, the time was recorded to obtain a running-average estimate of the walking speed. In all trials, the participants were free to adopt the most comfortable walking speed.

All different trials were randomly applied, except for the NO trial. This was due to the fact that placing this trial at the beginning or the end reduced the time needed for conducting the whole experiment and provided an invariant setup during the rest of the conditions. To have some different distribution among subjects, the NO trial was placed last for the four participants and first for the other three. The exact ordering of the trials for each subject is reported in Table 2.

During each trial, the subject followed an established sequence to reach steady state with oxygen consumption: 1 min sitting on a chair, 1 min in quiet standing, a 6-min WT, and 1 min in quiet standing until the $VO_2$ curve decreased back to steady state.

### Data Processing

For each subject, the following items were assessed:

- the kinematics during walking, i.e., the hip, knee, and ankle angular position among the different trials (from IMUs)
- the generated total reference torques, i.e., the outputs of the assistive controller
- the walking speed of the subject
- the normalized oxygen rate.

During each of the trials, the Oxycon device provided measurements of the oxygen uptake volume $VO_2$ in mL/min. These were normalized to body weight (BW) $W$ in kg and walking speed $v$ in m/min to obtain the oxygen cost per meter walked:

$$\text{Cost} = \frac{VO_2}{W \cdot v} \left[\frac{\text{mL}}{\text{kg} \cdot \text{m}}\right]. \tag{3}$$

An example of the $VO_2$ recordings normalized to BW for a representative subject is reported in Figure 5. When the 6-min WT starts, the $VO_2$ consequently begins to increase. After 2–3 min of walking, it stabilizes to a steady-state level.

The raw data were filtered with a running average filter over a span of five samples. For each of the trials, two intermediate minutes of the 6-min WT were kept for the analysis. This excluded the first 3 min, during which oxygen uptake did not reach steady state yet, as well as the last minute, which also showed transients at the end of the trial for some subjects. These last-minute transients were probably due to fluctuations in the measurement of the exact duration of the 6-min WT as well as the smoothing effect of the data filtering. The median value during the sitting-down phase and this steady-state 2-min interval were computed for further analyses.

To disregard potential fatigue effects over trials and to only focus on the extra oxygen cost required for walking, the $VO_2$ rates measured during walking were also normalized by subtracting from them the rates measured during the initial sitting-down condition. Finally, oxygen cost was further normalized to the TM trial, which represents 100%, and these results were averaged across all participants for each trial.

**The assistive trials managed to bring the subjects' metabolic rates to a condition in between NO and TM.**

To assess the impact of the assistive trials in the walking behavior and the metabolic cost, statistical t-tests were performed by individually comparing each of the assistive modes to the TM one with $p < 0.05$. These tests were performed to check significant changes in speed, cadence, and normalized oxygen cost.

## Results and Discussion

### Walking Kinematics

Participants walked at their preferred speed and with their preferred pattern during each of the trials. Figure 6(a) and (b) shows the average hip kinematics of all subjects in each of the trials. A reference from the literature [23] is also provided for qualitative comparison. The joint kinematics had very similar profiles across trials and to the one reported in [23]. This shows that, in principle, the assistance does not change the natural locomotion pattern of healthy participants. It also further illustrates the relevance of the computed primitives, since they were extracted from the literature data and followed the same kinematics as the participants.

The average speed and cadence during the 2-min interval of steady-state walking are shown in Figure 7. These variables are normalized with respect to the TM trial for each

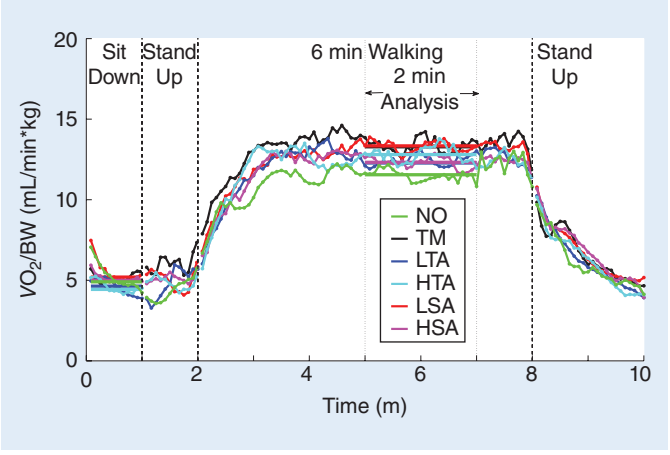


**Figure 5.** The smoothed oxygen uptake volume normalized to BW for S2 during each of the trials. The vertical lines represent the considered intervals for the data analysis. The horizontal lines represent the median values during the two analyzed intervals: sitting down and steady-state walking.

participant. The walking cadence was estimated from the frequency continuously learned by the AOs from the hip angular position. The average subject's cadence during the 2-min walking interval was thus computed as the median value of the average of the right and left legs' frequency over time.

We observed that wearing the device (with or without assistance) tended to make the subject walk more slowly than in the NO trial. This was correlated with a similar decrease in walking cadence. In general, the overall walking speed can be decreased (respectively increased) in two concurrent ways: either by decreasing (respectively increasing) the walking frequency or by decreasing (respectively increasing) the step length. It seems that our participants favored the former, although no direct measurement of the step length was available. Statistically significant differences for the walking speed with the NO trial were reached for the LTA and HTA trials ( $p = 0.0313$ and $p = 0.0137$, respectively). The same trials displayed a significant decrease in the walking cadence ($p = 0.0113$ and $p = 0.0084$, respectively). In sum, there was a significant reduction of both walking speed and cadence in the LTA and HTA trials. In the case of HSA, there was a significant reduction of the walking cadence with respect to the NO trial ($p = 0.0.0152$); however, the speed reduction did not reach significance ($p = 0.0533$). In the case of LSA, there was no significant reduction either in speed nor in cadence ($p = 0.1823$ and $p = 0.0710$, respectively). In any case, when comparing the TM mode with any of the assistive trials, there was no significant difference. Wearing the device caused the walking pace to decrease, and no change was observed between the nonassisted and assisted trials.

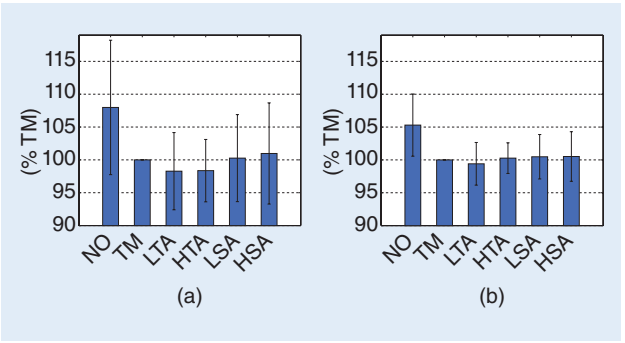


**Figure 7.** The (a) walking speed and (b) cadence mean values and standard deviations of the overall group for each of the trials, normalized to the TM trial.

Interestingly, this connects to a nice model-based prediction: if we assume that the subjects walk at their resonance frequency (i.e., the one that optimizes the exchanges between kinetic and potential energies), increasing their mass when wearing the APO should make this frequency decrease. Indeed, for a mass-spring system (which is often used as a very simplified model of walking [32]), the resonance frequency is proportional to $\sqrt{1/m}$. Therefore, it is logical to observe a decrease in walking cadence when the body mass is augmented, i.e., when the subject wears the device.

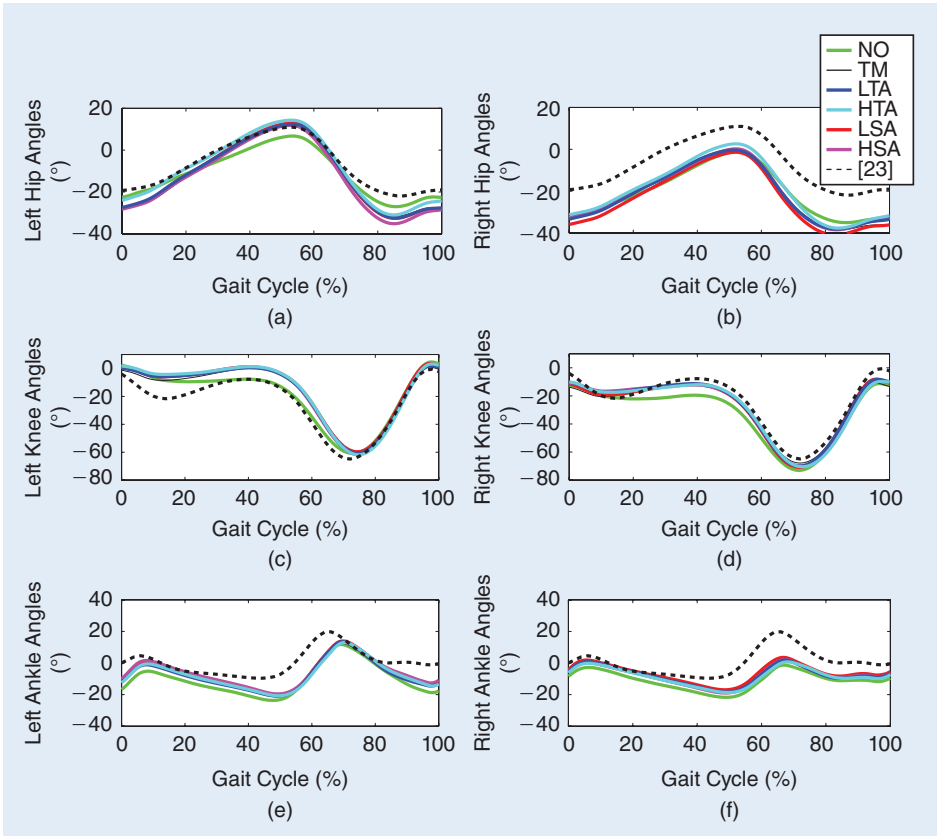


**Figure 6.** The kinematics of all joints during the 2 min of steady-state walking: (a) left hip, (b) right hip, (c) left knee, (d) right knee, (e) left ankle, and (f) right ankle. The colored solid lines represent the different trials the subjects underwent. The dashed black lines display data from [23] from the literature for comparison. Positive values represent extension, and negative values represent flexion. This figure shows data averaged across the healthy participants.

### *Walking Dynamics*

The average joint reference torques computed in the different trials are shown in Figure 8. In the case of NO, the APO was not worn by the subject, and, thus, no torque was provided. In the case of TM, the torque reference was set to zero, meaning that the powered orthosis was asked to follow the intended movement of the person without hindering it, i.e., with no

torque being delivered. In the case of the assistive modes, a fraction of these reference hip joint torques was provided, depending on the desired level of assistance.

In general, all computed torque reference profiles are similar to the ones found in the literature. This was expected, since these profiles were precisely generated by primitives constructed from the literature data. We can also observe an overall similarity between the torque profiles derived from the DLMP- and NLMP-based controllers. Again, this was expected, since healthy subjects have very similar kinematics to the ideal ones that were used to build the primitives. Nevertheless, some differences can be found between both approaches. Focusing on the hip, for example, the DLMP-based approach provided larger flexion torque than the NLMP-based approach, while the opposite holds for the extension torque. In addition, we can observe some divergence in the hip profiles after toe-off (between 65 and 85% of the gait cycle), where the NLMP-based control output shows a steep decrease in flexion followed by a plateau around zero torque, and the DLMP-based control output shows a smoother transition between flexion and extension torques.

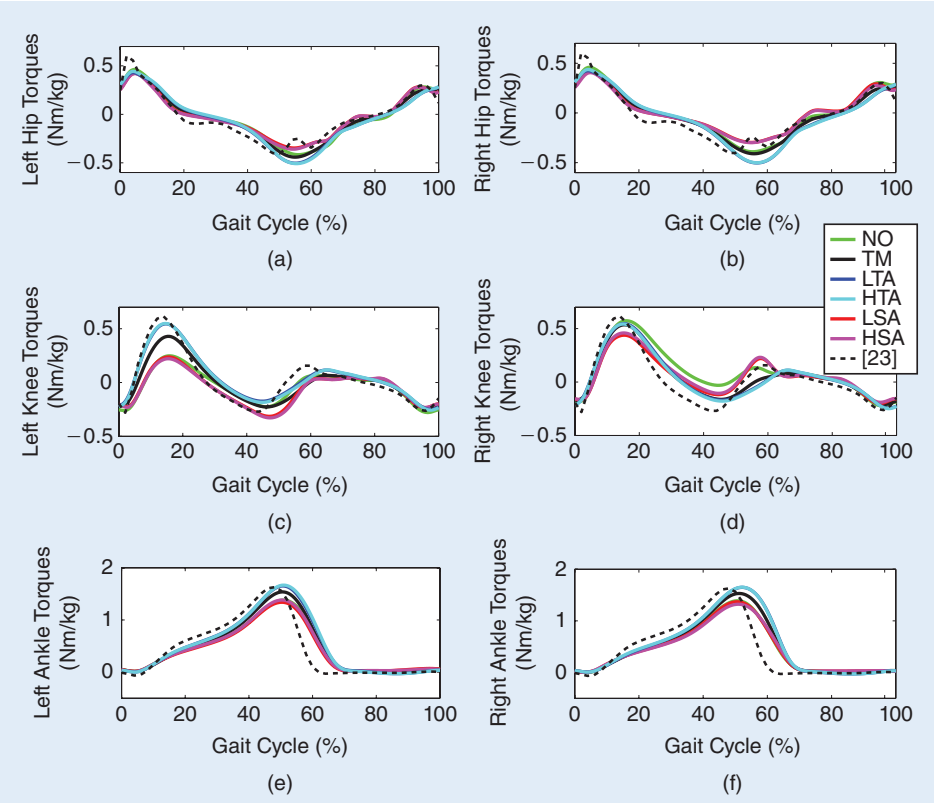


**Figure 8.** The reference torques of all joints during the 2 min of steady-state walking, normalized to BW: (a) left hip, (b) right hip, (c) left knee, (d) right knee, (e) left ankle, and (f) right ankle. The colored solid lines represent the different trials the subjects underwent. The dashed black lines display data from [23] from the literature for comparison. Positive values represent extension, and negative values represent flexion. This figure shows data averaged across healthy participants.

### *Oxygen Cost*

From the $VO_2$ uptake, the normalized oxygen cost of transportation was computed using (3) and the methods reported in the "Data Processing" section.

A possible fatigue effect within the 6-min WT was discarded because, for all considered subjects, there was no clear increasing trend of $O_2$ consumption with time during the trial (see, for example, the records for S2 in Figure 5).

Four of the seven subjects benefited from all the assistive trials. Two (S2 and S9) benefited from three of the four trials and displayed a small increment in the last one (less than 10%). Actually, this trial was the last to be tested for each of these two subjects, so they could have been impacted by fatigue across trials. One subject (S7) did not display a reduction in metabolic cost in any of the assistive conditions. For each subject that benefited from assistance, there was at least one assisted trial with more than 10% improvement with respect to TM. S1, S3, and S4 even presented trials displaying a decrease in oxygen cost with respect to the NO trial. In general, the assistive trials managed to bring the subjects' metabolic rates to a condition in between NO and TM, showing a decrease with respect to TM but still not enough to compensate for the payload of wearing the device.

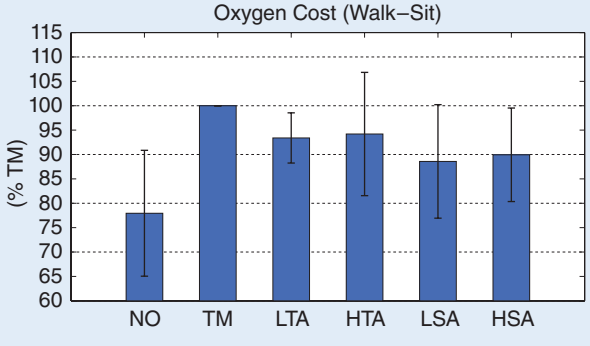


**Figure 9.** The oxygen rate mean values and standard deviations of the overall group for each of the trials, normalized to the TM.

The average cost data are shown in Figure 9, which displays a general increase in oxygen cost when moving from the

NO trial to the TM trial of about 22%. This increase was mainly due to the burden of wearing the 8.5-kg device, which was originally intended to be coupled to a leg orthosis and/or prosthesis, which could transfer a part of its weight directly to the ground. Nevertheless, a decrease in cost with respect to TM can be observed in any of the assistive modes, although standard deviations reveal large variability in the subject's adaptation during the different trials. t-tests of LTA, LSA, and HSA trials with respect to TM revealed significant reductions ($p = 0.0146$, $p = 0.0409$, and $p = 0.0322$, respectively). Only HTA did not reach significance ($p = 0.2704$). The oxygen cost decrease was the largest for the LSA and HSA trials, where it reached about 50% of the extra cost caused by wearing the device.

## Conclusion and Perspectives

In this article, a novel bioinspired controller based on motor primitives for locomotion assistance was developed. Based on data from the literature, a basic set of primitives was extracted that could reconstruct joint torques (by three DLMPs) or muscle stimulations (by six NLMPs) for walking cadences between 0.6 and 1 Hz and for ascending and descending stairs. The controller used this reduced set of primitive signals together with information from a WSA, i.e., the kinematics (joint angles) and ground reaction forces (swing/stance), to generate reference joint torques. This reduced set of sensors was directly attached to the user and, therefore, independent of the robot being used. This, together with the direct torque control output, makes the proposed control approach easily transferable to any torque-controlled assistive robot. This is especially true if we consider the NLMP-based control, which implements a virtual-musculoskeletal model. This controller naturally induces some adaptation to the subject's particular kinematics through artificial muscles but avoids the complex sensor deployment and signal processing required by EMG.

**Our method combined different mechanisms to continuously adapt the delivered torques to the subject's actual kinematics.**

To assess the assistive capability of both control approaches, several experiments were conducted. This included two analyses: the capability of the assistance to decrease the oxygen cost and the difference between using DLMP directly outputting torques or using NLMP and a musculoskeletal model.

Results on healthy walkers displayed between a 20 and 30% increase in metabolic cost when switching from the NO trial to TM, i.e., when the wearer is able to walk without encountering resistive actions from the orthosis. This reveals that the device weight had a significant negative impact on the subject cost of transport, despite all the efforts made to maximize its transparency. Nonetheless, the tested assistive methods proved to assist the subjects by reducing the oxygen cost with respect to TM, reaching a significant level for three of the four assistive trials. Therefore, it may be forecast that using a lighter exoskeleton would bring this reduction down to lower values than NO.

Our method combined different mechanisms to continuously adapt the delivered torques to the subject's actual kinematics. First, DLMPs were time-scaled as a function of the gait phase and frequency, being continuously and independently monitored for each leg by AOs. This opens the possibility to deliver nonsymmetrical patterns, a desirable feature for patients with hemideficits. Then, the primitives were multiplied by frequency-dependent weights, guaranteeing the adaptation of the torque profile to the current walking cadence. On top of that, NLMP generated stimulations that entered into a musculoskeletal model. This model captured a bioinspired muscle impedance, so that torques were generated not only as a function of the gait phase and walking frequency but also of the particular subject's kinematics. In brief, the generated torque adapts to the natural walking pattern of each different subject. Therefore, the NLMP approach should be more convenient for patients with pathologies causing the natural way of walking to differ from the ideal one of healthy subjects. Last but not least, this approach is more prone to integrate other bioinspired stimulations, such as reflexes or postural control [14].

Future work will focus on similar experiments with patients displaying a pathological gait to better assess the relevance of the NLMP-based method to adapt to each particular gait.

Finally, the system can easily be adjusted to convey the assistive strategy of a full orthosis or an active prosthesis. This can be done by following the same principles as the APO assistive strategy and adapting the outputs to the necessary control inputs of the device, if not directly torque driven.

## Acknowledgments

The authors would like to thank the Fondazione Don Carlo Gnocchi and especially Guido Pasquini and Federica Vannetti for their support with the recruitment of subjects, installations, and advice during the experiments.

This work was supported in part by the European Union within the CYBERLEGs project (FP7-ICT-2011-2.1 Grant 287894), by Fondazione Pisa within IUVO project 154/11, and the Belgian F.R.S.-FNRS (crédits aux chercheurs 6809010 to R. Ronsse, and travel grant to V. Ruiz Garate).

The two senior authors, listed last, contributed equally to cosupervise this work.

## References

[1] *World Population Ageing*, Department of Economic and Social Affairs, Population Division, United Nations, 2013.

[2] J. Verghese, A. LeValley, C. B. Hall, M. J. Katz, A. F. Ambrose, and R. B. Lipton, "Epidemiology of gait disorders in community-residing older adults," *J. American Geriatr. Soc.*, vol. 54, no. 2, pp. 255–261, 2006.

[3] T. Lenzi, M. C. Carrozza, and S. K. Agrawal, "Powered hip exoskeletons can reduce the users hip and ankle muscle activations during walking," *IEEE Trans. Neural Syst. Rehab. Eng.*, vol. 21, no. 6, pp. 938–948, 2013.

[4] M. R. Tucker, J. Olivier, A. Pagel, H. Bleuler, M. Bouri, O. Lambercy, J. R. Millan, R. Riener, H. Vallery, and R. Gassert, "Control strategies for active lower extremity prosthetics and orthotics: A review," *J. Neuroeng. Rehab.*, vol. 12, no. 1, 2015.

[5] I. Díaz, J. J. Gil, and E. Snchez, "Lower-limb robotic rehabilitation: Literature review and challenges," *J. Robot.*, vol. 2011, Article 759764, 11 pages, 2011.

[6] T. Yan, M. Cempini, C. M. Oddo, and N. Vitiello, "Review of assistive strategies in powered lower-limb orthoses and exoskeletons," *Robot. Autonomous Syst.*, vol. 64, pp. 120–136, Feb. 2015.

[7] W. Hassani, S. Mohammed, and Y. Amirat. (2013). Real-time emg driven lower limb actuated orthosis for assistance as needed movement strategy. in *Proc. Robotics: Science Systems Conf.* [Online]. Available: http://www.roboticsconference.org

[8] K. S. Türker, "Electromyography: Some methodological problems and issues," *Phys. Ther.*, vol. 73, no. 10, pp. 698–710, 1993.

[9] H. Kazerooni, J.-L. Racine, L. Huang, and R. Steger, "On the control of the Berkeley lower extremity exoskeleton (BLEEX)," in *Proc. IEEE Int. Conf. Robotics Automation*, 2005, pp. 4353–4360.

[10] A. J. Ijspeert, "Central pattern generators for locomotion control in animals and robots: A review," *Neural Netw.*, vol. 21, no. 4, pp. 642–653, 2008.

[11] S. Degallier and A. Ijspeert, "Modeling discrete and rhythmic movements through motor primitives: A review," *Biol. Cybern.*, vol. 103, no. 4, pp. 319–338, 2010.

[12] X. Zhang and M. Hashimoto, "Synchronization-based trajectory generation method for a robotic suit using neural oscillators for hip joint support in walking," *Mechatronics*, vol. 22, no. 1, pp. 33–44, 2012.

[13] R. Ronsse, T. Lenzi, N. Vitiello, B. Koopman, E. van Asseldonk, S. M. M. de Rossi, J. van den Kieboom, H. van der Kooij, M. C. Carrozza, and A. J. Ijspeert, "Oscillator-based assistance of cyclical movements: Model-based and model-free approaches," *Med. Biol. Eng. Comput.*, vol. 49, no. 10, pp. 1173–1185, 2011.

[14] H. Geyer and H. Herr, "A Muscle-reflex model that encodes principles of legged mechanics produces human walking dynamics and muscle activities," *IEEE Trans. Neural Syst. Rehab. Eng.*, vol. 18, no. 3, pp. 263–273, 2010.

[15] J. C. Selinger, S. M. O'Connor, J. D. Wong, and J. M. Donelan, "Humans can continuously optimize energetic cost during walking," *Curr. Biol.*, vol. 25, no. 18, pp. 2452–2456, 2015.

[16] E. Bizzi, V. C. K. Cheung, A. d'Avella, P. Saltiel, and M. Tresch, "Combining modules for movement," *Brain Res. Rev.*, vol. 57, no. 1, pp. 125–133, 2008.

[17] S. F. Giszter, "Motor primitives–new data and future questions," *Curr. opinion neurobiol.*, vol. 33, pp. 156–165, Aug. 2015.

[18] Y. P. Ivanenko, R. E. Poppele, and F. Lacquaniti, "Five basic muscle activation patterns account for muscle activity during human locomotion," *J. Physiol.*, vol. 556, pp. 267–282, Apr. 2004.

[19] G. Capellini, Y. P. Ivanenko, R. E. Poppele, and F. Lacquaniti, "Motor patterns in human walking and running," *J. Neurophysiol.*, vol. 95, no. 6, pp. 3426–3437, 2006.

[20] T. Flash and B. Hochner, "Motor primitives in vertebrates and invertebrate," *Curr. Opinion Neurobiol.*, vol. 15, no. 6, pp. 660–666, 2005.

[21] S. Degallier, L. Righetti, S. Gay, and A. Ijspeert, "Toward simple control for complex, autonomous robotic applications: Combining discrete and rhythmic motor primitives," *Autonomous Robot.*, vol. 31, no. 2, pp. 155–181, 2011.

[22] R. Ronsse, S. M. M. de Rossi, N. Vitiello, T. Lenzi, M. C. Carrozza, and A. J. Ijspeert, "Real-time estimate of velocity and acceleration of quasi-periodic signals using adaptive oscillators," *IEEE Trans. Robot.*, vol. 29, no. 3, pp. 783–791, 2013.

[23] D. A. Winter, The biomechanics and motor control of human gait: Normal, elderly and pathological, Ontario: Univ. of Waterloo Press, 1991.

[24] J. M. Wang, S. R. Hamner, S. L. Delp, and V. Koltun, "Optimizing locomotion controllers using biologically-based actuators and objectives," *ACM Trans. Graph.*, vol. 31, no. 4, Article 25, 2012.

[25] B. Koopman and W. van Dijk, "Basic gait kinematics: Reference data of normal subjects," Experimental data, Univ. of Twente, 2010.

[26] J. M. Bradford, D. A. Winter, "An integrated biomechanical analysis of normal stair ascent and descent," *J. Biomech.*, vol. 21, no. 9, pp. 733–744, 1988.

[27] R. Riener, M. Rabuffetti, and C. Frigo, "Stair ascent and descent at different inclinations," *Gait Posture*, vol. 15, no. 1, pp. 32–44, 2002.

[28] (2015, Mar. 28). CYBERLEGs. [Online]. Available: http://www.cyberlegs.eu/

[29] F. Giovacchini, F. Vannetti, M. Fantozzi, M. Cempini, M. Cortese, A. Parri, T. Yan, D. Lefeber, and N. Vitiello, "A light-weight active orthosis for hip movement assistance," *Robot. Autonomous Syst.*, vol. 73, pp. 123–134, Nov. 2014.

[30] L. Ambrozic, M. Gorsic, J. Geeroms, L. Flynn, R. Molino Lova, R. Kamnik, and M. Munih, N. Vitiello. "CYBERLEGs—A user-oriented robotic transfemoral prosthesis with whole–body awareness control," *IEEE Robot. Autom. Mag.*, vol. 21, no. 4, pp. 82–93, 2014.

[31] L. Righetti, J. Buchli, and A. J. Ijspeert. "Dynamic hebbian learning in adaptive frequency oscillators," *Physica D*, vol. 216, no. 2, pp. 269–281, 2006.

[32] H. Geyer, A. Seyfarth, and R. Blickhan, "Compliant leg behaviour explains basic dynamics of walking and running," *Proc. Biol. Sci.*, vol. 273, no. 1603, pp. 2861–2867, 2006.

***Virginia Ruiz Garate,*** Center for Research in Mechatronics; Institute of Mechanics, Materials, and Civil Engineering; and Louvain Bionics, Université catholique de Louvain, Louvain-la-Neuve, Belgium. E-mail: virginia.ruizgarate@uclouvain.be.

***Andrea Parri,*** The BioRobotics Institute, Scuola Superiore Sant'Anna, Pisa, Italy. E-mail: an.parri@sssup.it.

***Tingfang Yan,*** The BioRobotics Institute, Scuola Superiore Sant'Anna, Pisa, Italy. E-mail: t.yan@sssup.it.

***Marko Munih,*** Laboratory of Robotics, Faculty of Electrical Engineering, University of Ljubljana, Slovenia. E-mail: marko.munih@robo.fe.uni-lj.si.

***Raffaele Molino Lova,*** Fondazione Don Carlo Gnocchi, Firenze, Italy. E-mail: rmolino@dongnocchi.it

***Nicola Vitiello,*** The BioRobotics Institute, Scuola Superiore Sant'Anna, Pisa, Italy; and Fondazione Don Carlo Gnocchi, Firenze, Italy. E-mail: n.vitiello@sssup.it

***Renaud Ronsse,*** Center for Research in Mechatronics; Institute of Mechanics, Materials, and Civil Engineering; and Louvain Bionics, Université catholique de Louvain, Louvain-la-Neuve, Belgium. E-mail: renaud.ronsse@uclouvain.be.